Electronic Supplementary Material (ESI) for Analytical Methods.

Electronic Supplementary Information

Rapid detection of silver ions based on luminescent carbon nanodots for multicolor patterning, smartphone sensors, and bioimaging applications

Sonaimuthu Mohandoss,[a] Subramanian Palanisamy,[b] SangGuan You,[b] Jae-Jin Shim[a] and Yong Rok Lee*[a]

[a]School of Chemical Engineering, Yeungnam University, Gyeongsan, Gyeongbuk-do 38541, Republic of Korea.

[b]Department of Marine Food Science and Technology, Gangneung-Wonju National University, 120 Gangneungdaehangno, Gangneung, Gangwon 25457, Republic of Korea.

*Corresponding author: Yong Rok Lee (*E-mail*: yrlee@yu.ac.kr).

Materials

2,4-Diaminobenzenesulfonic acid (2,4-DABSA) was obtained from Sigma-Aldrich. All metal ion stock solutions were prepared from metal nitrate or perchlorate salts were purchased from Sigma - Aldrich. The organic solvents of acetone, acetonitrile, diethyl ether, 1,4-dioxane, N, N-dimethylformamide, dimethyl sulfoxide, ethanol, ethyl acetate, and methanol were purchased from Sigma-Aldrich and TCI. The experiments were carried out in HEPES buffer solution (10 mM pH = 7.4). All other experimental chemicals were of analytical grade and used directly without further purification.

Characterization of N,S-CNDs

The molecules were registered with a UV 3220 spectrometer (Optizen) or a spectrometer (HITACHI) F-2700 with a Xe Arc Lamp in ultraviolet-visible (UV–Vis) and fluorescence spectra respectively. The pH values of solutions were measured using 720P pH meter (Istek instruments). The FT-IR spectra were recorded using an FT-IR spectrometer (Perkin Elmer) in the range of 4000–400 cm^{-1}. The diffraction study was conducted using a 5° min^{-1} scanning speed with a wavelength of 1,5405 Å was performed with a 10-80° range of X-ray diffractometer (XRD) (PANalytic X'Pert Philips, MRD model). Raman spectroscopy was performed to investigate the SERS behaviors of substrates using a Raman (Horiba HR Evolution 800) spectrometer with 532 nm laser wavelength, 48 mW laser power, 1200 gr/mm diffraction grid, and 500 nm spatial resolution at the core research support center for natural products and medical materials, Yeungnam University. X-ray photoelectron spectroscopy (XPS, Thermo Fisher, USA.) measurements were obtained using Multilab-2000 spectrometer with Al Kα radiation monochromatized source. High-resolution and transmission electron microscopy (HRTEM and

TEM) images were recorded (JEOL JEM-2100) with an accelerating voltage of 200 kV. The specimens used for TEM were prepared by evaporating one drop of the sample solution on lacy grids, followed by drying at room temperature.

Calculation of the photoluminescence quantum yield

The N,S-CNDs solution was diluted to keep the absorption intensity below 0.1 and the excitation wavelength set to 370 nm. After that, solutions for absorption and emission measurements were carried out in a 1 x 1 cm quartz cuvette. Quantum yield (QY) was measured using a fluorescence spectrophotometer F-7000 (Hitachi). Photoluminescence QY can be calculated using the following equation:

$$QY = \frac{\int L_{emission}}{\int E_{solvent} - \int E_{sample}}$$

Here, QY was the quantum yield and $L_{emission}$ was the photoluminescence emission spectrum of the N,S-CNDs sample. E_{sample} was the spectrum of light used to excite the sample and $E_{solvent}$ was the spectrum of light used to excite only the solvent of the sphere, collected using a sphere. The solvent in this experiment was a pH 7.4 buffer.

PL stability optimization

N,S-CND solutions (50 μg/mL) were prepared using different solvents, buffer solutions (pH 1–13), salt ionic strength (NaCl, 0.5–10 M), and time optimization (1–120 min). The photoluminescence spectra were measured at excitation and emission wavelength of 370 nm and 380–700 nm, respectively.

Photoluminescence stability of N,S-CNDs

To verify the stability of N,S-CND, we measured the effects of representative solvents, pH levels, ionic strength, long-term illumination, and storage time on PL intensity. The synthesized N,S-CNDs were dissolved in acetone, acetonitrile, diethyl ether, 1,4-dioxane, N, N-dimethylformamide, dimethyl sulfoxide, ethanol, ethyl acetate, methanol, and water to investigate the effect of solvent-dependent PL emission behavior and their color changes as shown in Fig. S1.[1] Owing to their characteristics, N,S-CNDs can emit strong PL in hydrophilic solvents such as water, ethanol, and methanol. This indicates that the synthesized N,S-CNDs do not interfere with PL activity and exhibit high solubility in widely used solvents. The solvatochromism of N,S-CNDs induced a charge transfer process involved in the photophysical process of the N,S-CNDs.[2] A large blue shift was observed between the N,S-CNDs in N, N-dimethylformamide and N,S-CNDs in other organic solvents. In addition, increasing the ionic strength of the N,S-CNDs aqueous solution by incrementally adding NaCl did not affect the PL intensity even when the concentration of NaCl was 1.0 M, revealing its outstanding stability under high saline conditions (Fig. S2a).[3] As illustrated in Fig. S2b, the N,S-CNDs exhibited a stable PL within a wide pH range (e.g., pH 6–8), which was selected as the optimum pH level. However, in a strongly acidic (pH < 2) or basic medium (pH > 10), a sharp decrease in the PL intensity was observed. The intensity of the N,S-CNDs was 95% of the maximum when its pH was 7.0. This confirmed that N,S-CNDs could be used in biomedical applications because the physiological pH is 7.4. N,S-CNDs were colorless in daylight and showed bright blue PL under 365 nm UV irradiation in aqueous solution (Fig. S2c,d). The PL intensity was very stable with increasing time upto 120 min at 370 nm (Fig. S3a). This was further confirmed by a remarkably constant PL intensity of N,S-CNDs decreased to less than 5%

after 6 months (Fig. S3b).[4] This property is important because the synthesized N,S-CNDs must be water-soluble and stable in the surrounding environment for use in sensing applications. The overall stability optimization results showed that the PL intensity of N,S-CNDs was significantly stable with various solvents polarity, a wide range of pH values from 6 to 8, and ultra-high concentration of NaCl solution up to 10 M, and at continuous irradiation time up to 120 min (Figs. S1-S3).

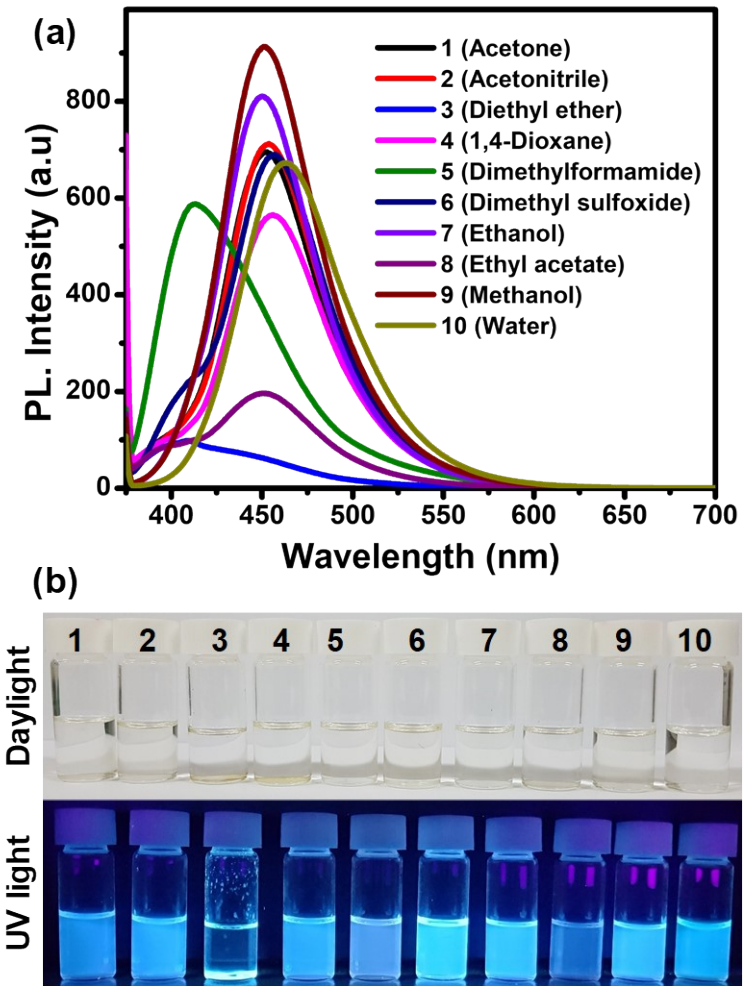

Figure S1. (a) PL emission spectra of N,S-CNDs (50 µg/mL) suspensions in various solvents under an excitation of 370 nm. (b) PL color changes of N,S-CNDs (50 µg/mL) suspensions in (1) Acetone, (2) Acetonitrile, (3) Diethyl ether, (4) 1,4-Dioxane, (5) Dimethylformamide, (6)

Dimethyl sulfoxide, (7) Ethanol, (8) Ethyl acetate, (9) Methanol, and (10) Water in daylight (top) under UV lamp at 365 nm irradiation (bottom).

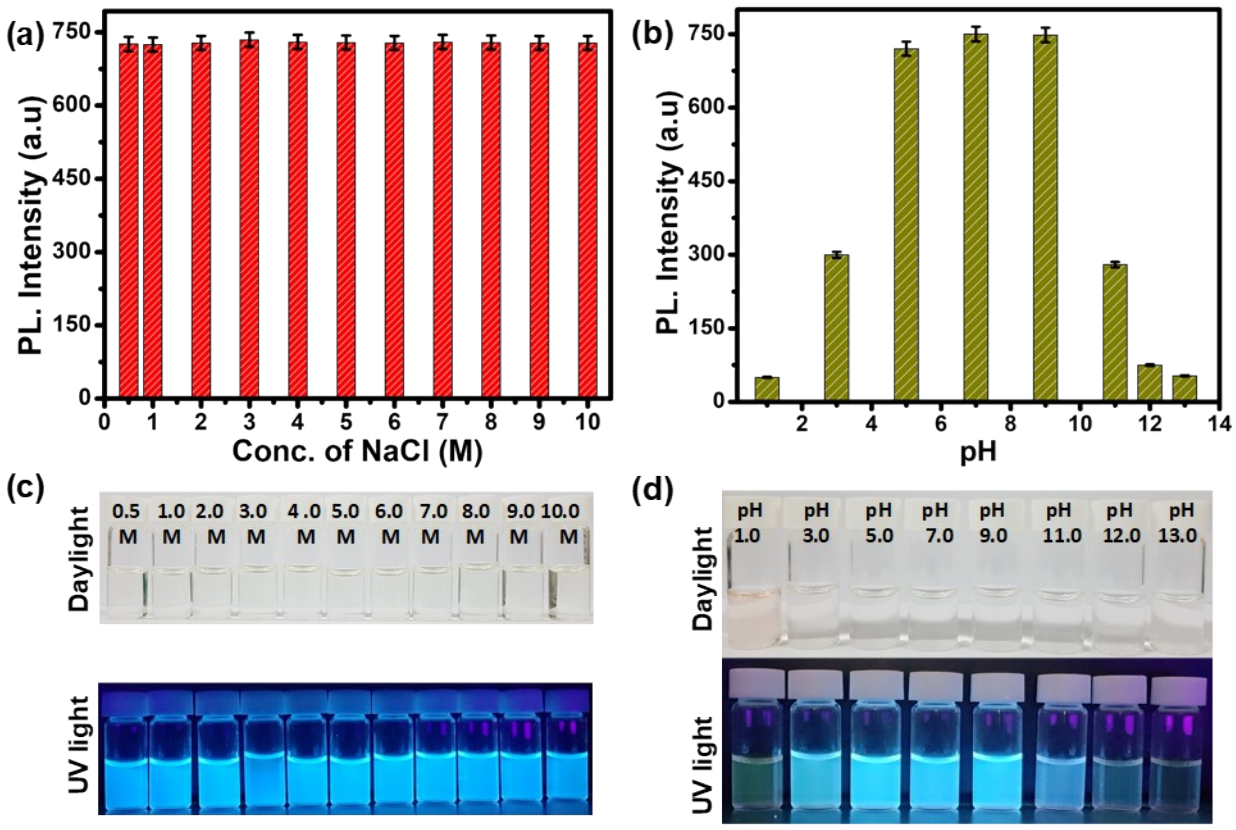

Figure S2. PL stability of N,S-CNDs (50 µg/mL) suspension in various concentration of (a) NaCl; 0.5–10 M and (b) pH~1.0 – 13.0; (λ_{ex} = 370 nm). PL color changes of N,S-CNDs (50 µg/mL) suspensions in various concentration of (c) NaCl; 0.5–10 M and (d) pH~1.0 – 13.0 in daylight (top) under UV lamp at 365 nm irradiation (bottom).

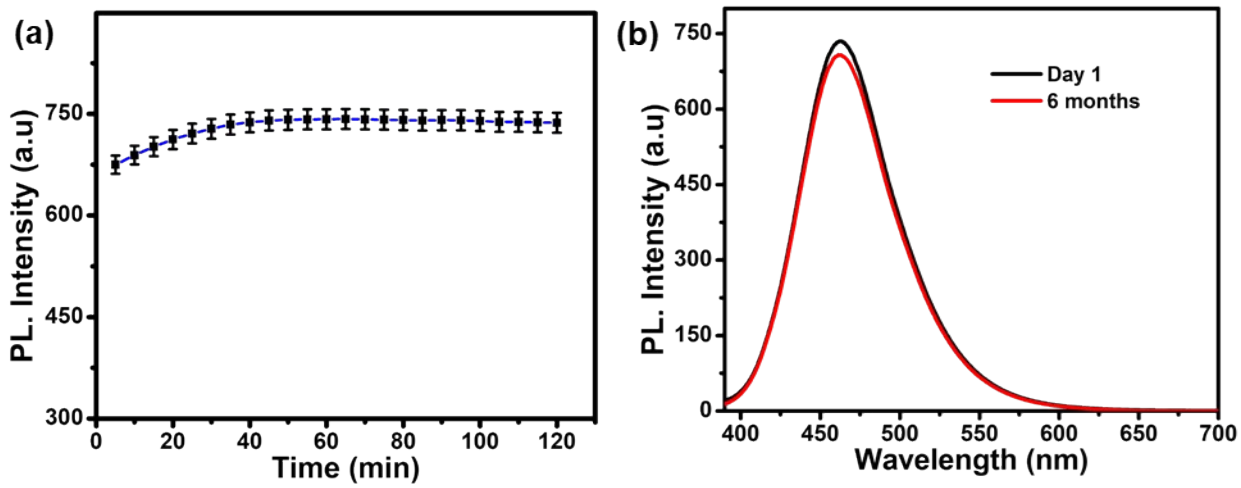

Figure S3. (a) Reaction time variation and (b) Long time storage stability of PL N,S-CNDs (50 µg/mL) suspension in HEPES buffer solution (10 mM; pH = 7.4), (λ_{ex} = 370 nm; λ_{em} = 463 nm).

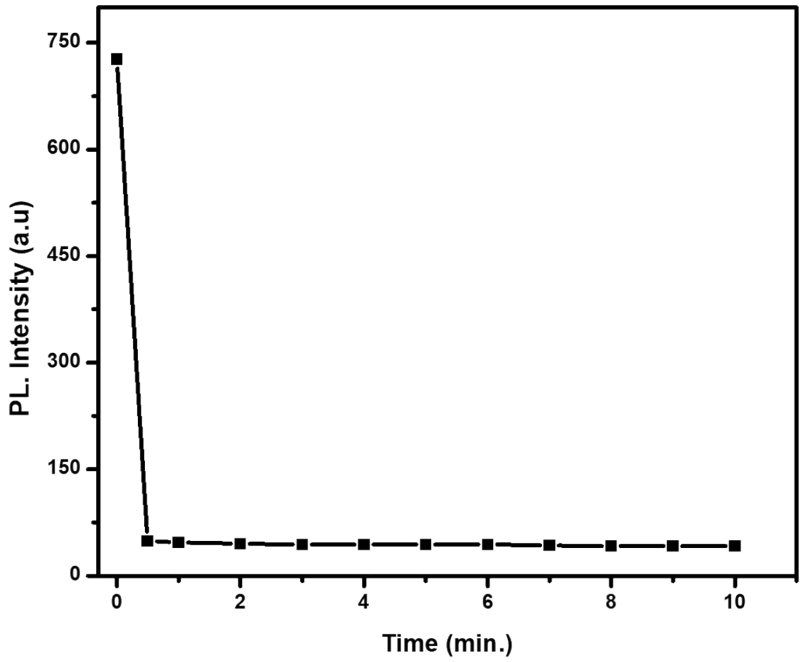

Figure S4. The time dependence of N,S-CNDs (50 µg/mL) PL sensor on detection of Ag^{+} (3.0 µM) in HEPES buffer solution (10 mM; pH = 7.4), (λ_{ex} = 370 nm; λ_{em} = 463 nm and 480 nm).

Interference effects of Ag^+ ions using cations and anions

To further investigate the tolerance to Ag^+ over other cations and anions, a competition experiment was accomplished by mixing N,S-CNDs/Ag^+ with various coexistent cations and anions. We investigated the PL behavior of N,S-CNDs to a variety of cations like Ba^{2+}, Ca^{2+}, Cd^{2+}, Ce^{3+}, Cu^{2+}, Co^{2+}, Fe^{3+}, Hg^{2+}, Mn^{2+}, Na^+, Ni^{2+}, Pb^{2+}, Sn^{2+}, Sr^{2+}, Ti^{3+}, and Zn^{2+} (100 μM) and anions like $Br^–$, $Cl^–$, $ClO_4^–$, $CO_3^{2–}$, $I^–$, $OH^–$, $NO_2^–$, $NO_3^{2–}$, $H_2PO_4^–$, $HPO_4^{2–}$, $PO_4^{3–}$, HSO_3^-, SO_3^{2-}, SO_4^{2-}, $S_2O_4^{2-}$, $S_2O_8^{2-}$, and S^{2-} in HEPES buffer solution (10 mM; pH = 7.4), (λ_{ex} = 370 nm; λ_{em} = 463 nm and 480 nm). As shown by the PL spectra, the N,S-CNDs were particularly sensitive and selective to Ag^+ ions even in the presence of a higher concentration of up to 100 μM of other cations and anions (Figs. S5 and S6). No difference in the PL intensity at 463 nm and 480 nm between the experimental cations and anions of equivalent aliquots was observed. As shown in Fig. S7, the addition of Ag^+ to N,S-CNDs resulted in a significantly decreased PL, but other cations and anions showed little or no change in PL intensity compared to free N,S-CNDs. Thus, the presence of other cations and anions does not interfere with the detection of Ag^+. These findings demonstrated that even in the presence of interfering cations and anions, N,S-CNDs showed high selectivity and stability toward Ag^+ ions.

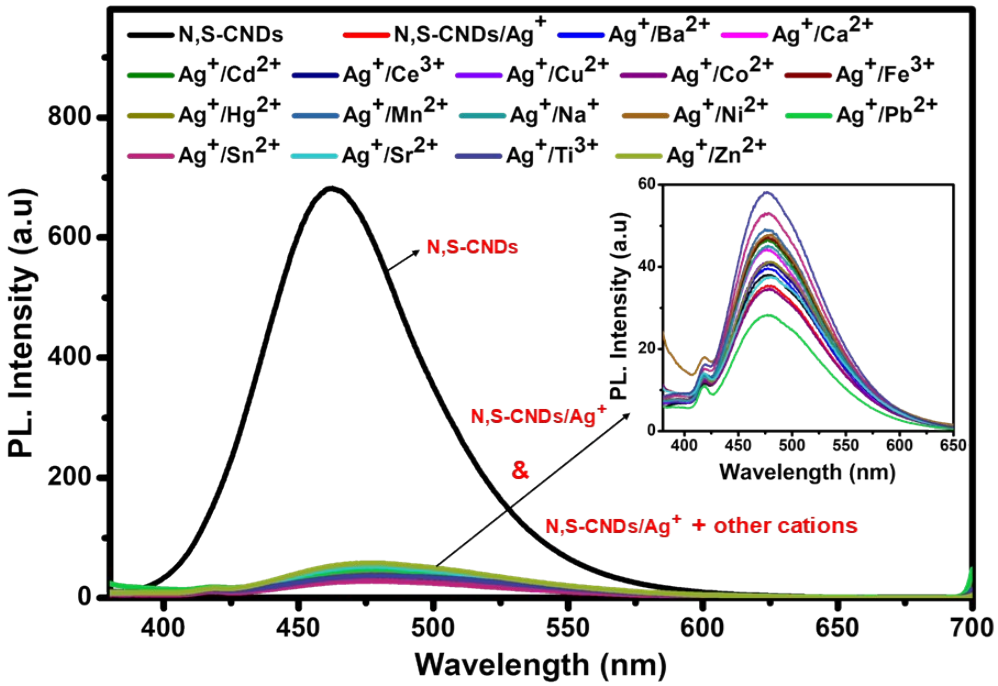

Figure S5. (a) PL spectra of the N,S-CNDs/Ag^{+} (N,S-CNDs; 50 μg/mL and Ag^{+}; 3.0 μM) with the addition of various cations (Ba^{2+}, Ca^{2+}, Cd^{2+}, Ce^{3+}, Cu^{2+}, Co^{2+}, Fe^{3+}, Hg^{2+}, Mn^{2+}, Na^{+}, Ni^{2+}, Pb^{2+}, Sn^{2+}, Sr^{2+}, Ti^{3+}, and Zn^{2+}; 100 μM) in HEPES buffer solution (10 mM; pH 7.4) (λ_{ex} = 370 nm; λ_{em} = 480 nm).

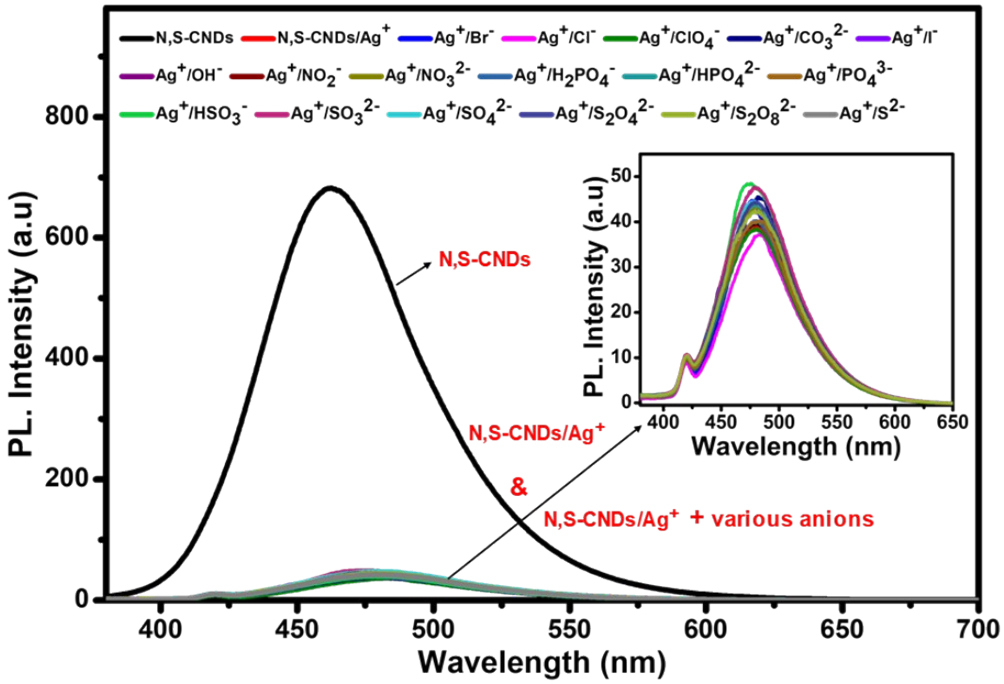

Figure S6. (a) PL spectra of the N,S-CNDs/Ag^{+} (N,S-CNDs; 50 μg/mL and Ag^{+}; 3.0 μM) with the addition of various anions (Br^{-}, Cl^{-}, ClO_4^{-}, CO_3^{2-}, I^{-}, OH^{-}, NO_2^{-}, NO_3^{2-}, $H_2PO_4^{-}$, HPO_4^{2-}, PO_4^{3-}, HSO_3^{-}, SO_3^{2-}, SO_4^{2-}, $S_2O_4^{2-}$, $S_2O_8^{2-}$, and S^{2-}; 100 μM) in HEPES buffer solution (10 mM; pH 7.4) (λ_{ex} = 370 nm; λ_{em} = 480 nm).

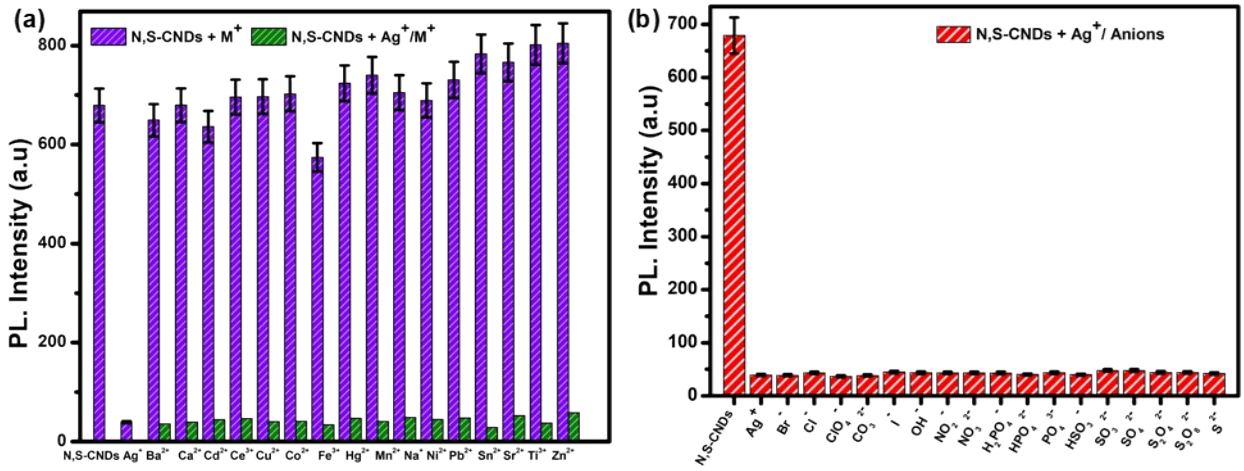

Figure S7. Competition graph of the N,S-CNDs/Ag^{+} (N,S-CNDs; 50 µg/mL and Ag^{+}; 3.0 µM) with the addition of (a) various cations (Ba^{2+}, Ca^{2+}, Cd^{2+}, Ce^{3+}, Cu^{2+}, Co^{2+}, Fe^{3+}, Hg^{2+}, Mn^{2+}, Na^{+}, Ni^{2+}, Pb^{2+}, Sn^{2+}, Sr^{2+}, Ti^{3+}, and Zn^{2+}; 100 µM) and (b) various anions (Br^{-}, Cl^{-}, ClO_4^{-}, CO_3^{2-}, I^{-}, OH^{-}, NO_2^{-}, NO_3^{2-}, $H_2PO_4^{-}$, HPO_4^{2-}, PO_4^{3-}, HSO_3^{-}, SO_3^{2-}, SO_4^{2-}, $S_2O_4^{2-}$, $S_2O_8^{2-}$, and S^{2-}; 100 µM) in HEPES buffer solution (10 mM; pH 7.4). The violet bars represent the addition of an excess of the appropriate metal ions (3.0 µM) to N,S-CNDs (50 µg/mL) solution. The green bars represent the subsequent addition of 3.0 µM Ag^{+} with cations (100 µM) to N,S-CNDs (50 µg/mL) solution. The red bars represent the subsequent addition of 3.0 µM Ag^{+} with anions (100 µM) to N,S-CNDs (50 µg/mL) solution. (λ_{ex} = 370 nm; λ_{em} = 463 nm and 480 nm).

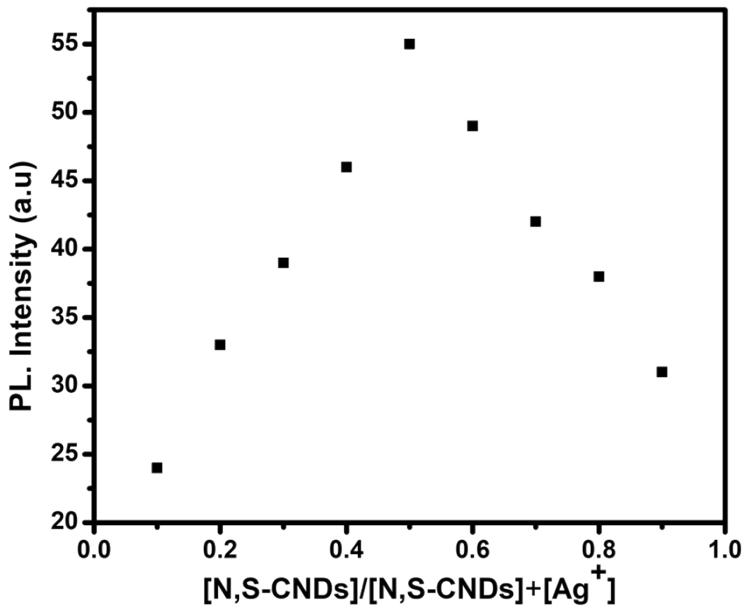

Figure S8. Jobs plot suggesting stoichiometry among PL sensor N,S-CNDs and Ag^+ = 1:1. (N,S-CNDs; 50 μg/mL and Ag^+; 3.0 μM) in HEPES buffer solution (10 mM; pH = 7.4), (λ_{ex} = 370 nm; λ_{em} = 480 nm).

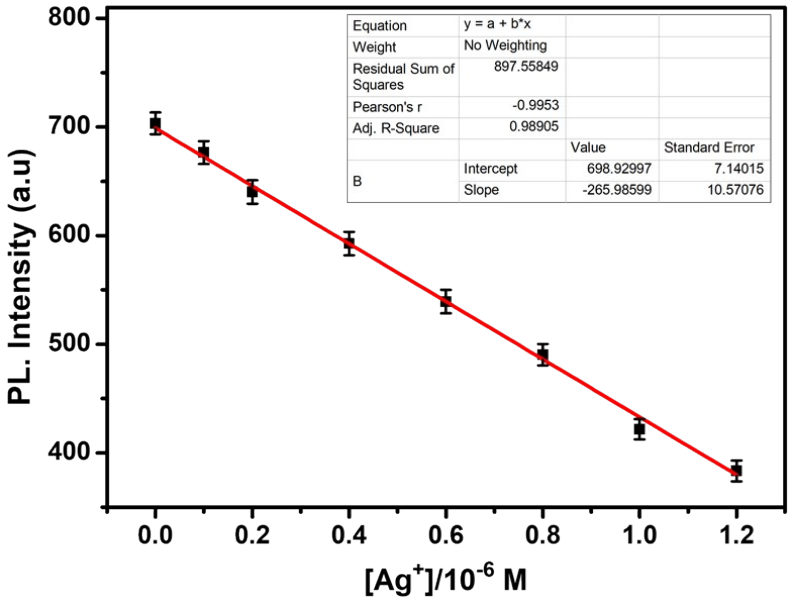

Figure S9. Calibration curve of N,S-CNDs in the presence of Ag^{+} ions. (N,S-CNDs; 50 µg/mL and Ag^{+}; 3.0 µM) in HEPES buffer solution (10 mM; pH = 7.4), (λ_{ex} = 370 nm; λ_{em} = 463 nm). The limit of detection (LOD) of Ag^{+} was determined from the following equation: LOD = K × SD/S, where K = 3; SD is the standard deviation of the blank solution; S is the slope of the calibration curve. LOD (Ag^{+}) = K × SD/S = 3 × 0.6989/265.98 x 10^{-6} M= 0.00788× 10^{-6} M = 7.88 × 10^{-9} M.

Table S1. The performance of various fluorescent carbon dots probe for Ag^+ ion detection.

Materials	**Methods**	**Linear range (μM)**	**LOD**	**Ref.**
CNDs	Fluorescence	0–90	320 nM	5
CDs	UV–vis	0–100	26 nM	6
S,N-CQDs	Fluorescence	0–250	0.4 μM	7
CQDs	Fluorescence	0 – 600	0.5 μM	8
S-GQDs	Fluorescence	0.1–130	30 nM	9
CdTe QDs	Fluorescence	0.08–0.6	0.01 μM	10
Cys-CdS QDs	Fluorescence	0.1–1.5	68 nM	11
N-H-CQDs	Fluorescence	0–100	21 nM	12
CDs	Fluorescence	0–45	15 nM	13
CDs	Fluorescence	0.1–25	37 nM	14
N-CQDs	Fluorescence	0.2–40	0.168 μM	15
CDs	Fluorescence	5.0 –100	1400 μM	16
NBS-CDs	Fluorescence	0–0.30	0.35 μM	17
ASL/GQDs	Fluorescence	0–0.50	4.7 μM	18
NCDs	Fluorescence	1–100	1.0 μM	19
N,S-CNDs	Photoluminescence	0– 1.2	7.88 nM	This work

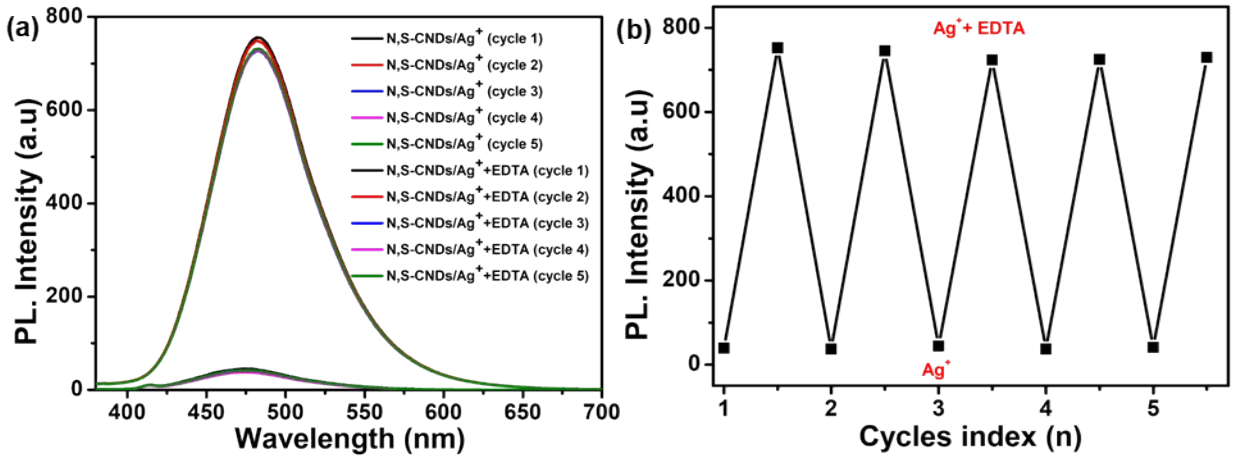

Figure S10. Reversible changes of N,S-CNDs (50 μg/mL) after the sequential addition of Ag^+ ions (3.0 μM) and EDTA (30 μM) in HEPES buffer solution (10 mM; pH = 7.4) (λ_{ex} = 370 nm; λ_{em} = 480 nm).

Determination of Ag^+ in environmental water samples

Samples of lake and tap water were collected from Gyeongsan High School premises and our laboratory (Yeungnam University), South Korea, respectively. All the water samples were firstly centrifuged at 10000 rpm for 30 min followed by filtration (0.22 μm cellulose membrane) to remove any suspensions before preparing the spiked solutions. The residual chlorine in tap water sample was removed by heating to boiling. The recovery rates of Ag^+ based on this N,S-CNDs sensing system were calculated by adding the series concentrations of Ag^+ standard solutions into the different environmental water samples.

Table S2. Application of PL sensor N,S-CNDs towards Ag^+ recovery in water samples

Samples	Ag^+ added (μM)	Ag^+ found (μM)	Recovery (%)	RSD (%)
Tap water	0.5	0.49	98.0	1.35
	1.0	1.04	104.0	4.21
	2.0	2.11	105.5	2.18
Lake water	0.5	0.53	106.0	4.48
	1.0	1.05	105.0	2.27
	2.0	2.11	105.5	3.98

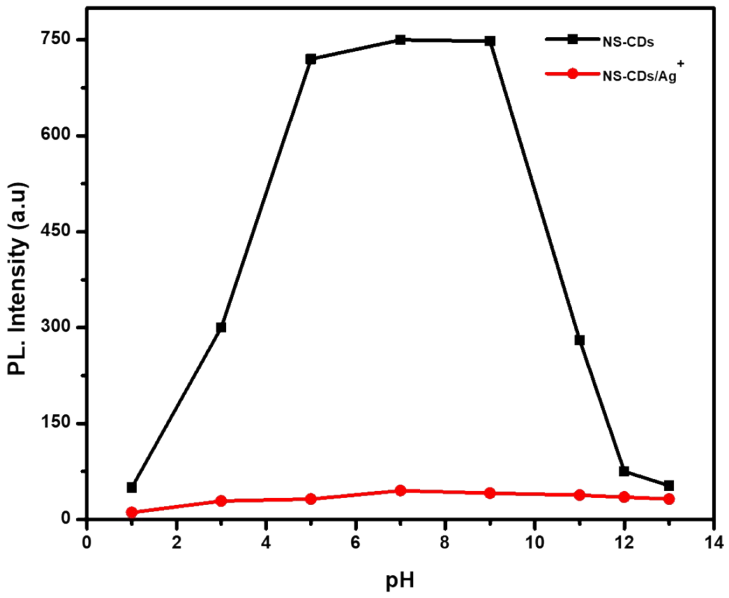

Figure S11. The pH influence of PL N,S-CNDs intensity in the presence of Ag^{+}. (N,S-CNDs; 50 µg/mL and Ag^{+}; 3.0 µM) in HEPES buffer solution (10 mM; pH = 7.4), (λ_{ex} = 370 nm; λ_{em} = 463 nm/480 nm).

References

1 X. Shi, Y. Hu, H. M. Meng, J. Yang, L. Qu, X. B. Zhang and Z. Li, *Sens Actuators B Chem*, 2020, **306**, 127582.

2 A. Ekbote, S.M. Mobin, R. Misra, *J Mater Chem C*, 2020, **8**, 3589–3602.

3 S. W. Huang, Y. F. Lin, Y. X. Li, C. C. Hu and T. C. Chiu, *Molecules*, 2019, **24**, 1–12.

4 L. Li, L. Shi, J. Jia, O. Eltayeb, W. Lu, Y. Tang, C. Dong and S. Shuang, *Sens Actuators B Chem*, 2021, **332**, 129513.

5 X. Gao, Y. Lu, R. Zhang, S. He, J. Ju, M. Liu, L. Li and W. Chen, *J Mater Chem C*, 2015, **3**, 2302–2309.

6 J. C. Jin, B. B. Wang, Z. Q. Xu, X. H. He, H. F. Zou, Q. Q. Yang, F. L. Jiang and Y. Liu, *Sens Actuators B Chem*, 2020, 2018, **267**, 627–635.

7 S. Liao, X. Zhao, F. Zhu, M. Chen, Z. Wu, X. song, H. Yang and X. Chen, *Talanta*, 2018, **180**, 300–308.

8 N. Arumugam and J. Kim, *Mater Lett*, 2018, **219**, 37–40.

9 S. Bian, C. Shen, Y. Qian, J. Liu, F. Xi and X. Dong, *Sens Actuators B Chem*, 2017, **242**, 231–237.

10 J. H. Wang, H. Q. Wang, H. L. Zhang, X. Q. Li, X. F. Hua, Y. C. Cao, Z. L. Huang and Y. Di Zhao, *Anal Bioanal Chem*, 2007, **388**, 969–974.

11 T. Khantaw, C. Boonmee, T. Tuntulani and W. Ngeontae, *Talanta*, 2013, **115**, 849–856.

12 X. Jiang, J. Huang, T. Chen, Q. Zhao, F. Xu and X. Zhang, *IntJBiolMacromol*,2020,**153**, 412–420.

13 J. Guo, S. Ye, H. Li, J. Song and J. Qu, *Dyes Pigm*, 2020, **183**, 108723.

14 H. Lu, C. Li, H. Wang, X. Wang and S. Xu, *ACS Omega*, 2019, **4**, 21500–21508.

15 R. Tabaraki and A. Nateghi, *J Fluoresc*, 2016, **26**, 297–305.

16 Y. Ma, W. Lv, Y. Chen, M. Na, J. Liu, Y. Han, S. Ma and X. Chen, *New J Chem*, 2019, **43**, 5070–5076.

17 L. Xu, X. Yang, H. Ding, S. Li, M. Li, D. Wang and J. Xia, *Mater Sci Eng C*, 2019, **102**, 917–922.

18 S. Huang, E. Yang, J. Yao, Y. Liu and Q. Xiao, *Anal Chim Acta*, 2018, **1035**, 192–202.

19 Z. Qian, J. Ma, X. Shan, H. Feng, L. Shao and J. Chen, *Chem Eur J*, 2014, **20**, 2254–2263.